New Phytologist

Methods

Characterizing natural variability of lignin abundance and composition in fine roots across temperate trees: a comparison of analytical methods

Mengxue Xia[1], Oscar J. Valverde-Barrantes[2], Vidya Suseela[1], Christopher B. Blackwood[3] and Nishanth Tharayil[1]

[1]Department of Plant & Environmental Sciences, Clemson University, Clemson, SC 29634, USA; [2]International Center for Tropical Biodiversity, Institute of Environment, Florida International University, Miami, FL 33199, USA; [3]Department of Biological Sciences, Kent State University, Kent, OH 44242, USA

Authors for correspondence:
Mengxue Xia
Email: xiamengxue12@gmail.com

Nishanth Tharayil
Email: ntharay@clemson.edu

Received: *6 March 2022*
Accepted: *27 August 2022*

New Phytologist (2022) **236:** 2358–2373
doi: 10.1111/nph.18515

Key words: acid-insoluble fraction, cupric oxide (CuO) oxidation, fine roots, Fourier transform infrared (FTIR) spectroscopy, lignin, pyrolysis–gas chromatography–mass spectrometry (py-GC-MS), root chemical traits, thioacidolysis.

Summary

- Lignin is an important root chemical component that is widely used in biogeochemical models to predict root decomposition. Across ecological studies, lignin abundance has been characterized using both proximate and lignin-specific methods, without much understanding of their comparability. This uncertainty in estimating lignin limits our ability to comprehend the mechanisms regulating root decomposition and to integrate lignin data for large-scale syntheses.
- We compared five methods of estimating lignin abundance and composition in fine roots across 34 phylogenetically diverse tree species. We also assessed the feasibility of high-throughput techniques for fast-screening of root lignin.
- Although acid-insoluble fraction (AIF) has been used to infer root lignin and decomposition, AIF-defined lignin content was disconnected from the lignin abundance estimated by techniques that specifically measure lignin-derived monomers. While lignin-specific techniques indicated lignin contents of 2–10% (w/w) in roots, AIF-defined lignin contents were *c.* 5–10-fold higher, and their interspecific variation was found to be largely unrelated to that determined using lignin-specific techniques. High-throughput pyrolysis–gas chromatography–mass spectrometry, when combined with quantitative modeling, accurately predicted lignin abundance and composition, highlighting its feasibility for quicker assessment of lignin in roots.
- We demonstrate that AIF should be interpreted separately from lignin in fine roots as its abundance is unrelated to that of lignin polymers. This study provides the basis for informed decision-making with respect to lignin methodology in ecology.

Introduction

Fine roots play a critical role in plant fitness and biogeochemical cycles in terrestrial ecosystems (Freschet *et al.*, 2013; Gherardi & Sala, 2020). By maintaining a large surface area and intimate contact with soil, fine roots acquire essential soil resources for plants. The plasticity of fine roots, morphologically and/or chemically, is often the key adaptive response of trees to the ever-changing availability of water and nutrients (Chen *et al.*, 2016; Suseela *et al.*, 2020). At a broader scale, fine roots dominate carbon input to soil and regulate terrestrial carbon and nutrient cycling. The turnover of fine roots channels *c.* 46% of global terrestrial carbon (C) fixation to the soil (Gherardi & Sala, 2020). This large amount of root C is partly transformed into soil organic carbon via root decomposition and is estimated to contribute two-fold more to soil carbon storage than aboveground plant parts (Rasse *et al.*, 2005).

Lignin is a class of complex biopolymers which are formed by combinatorial coupling of phenylpropane units (primarily consisting of *p*-hydroxyphenyl or H, guaiacyl or G, syringyl or S, Ralph *et al.*, 2004). Lignin is deposited in the cell wall of vascular plants and provides structural integrity to plant tissues (Boerjan *et al.*, 2003). It is also an important component of fine roots that influences many of their ecological roles, such as resource acquisition and decomposition. The accumulation of lignin in roots may enhance root tensile strength that facilitates soil exploration (Schneider *et al.*, 2021) and can form diffusion barriers that control solute and water balance (Reyt *et al.*, 2021). Lignin abundance has also been empirically established as a major factor regulating root decomposition, where higher initial lignin content was associated with slower decomposition (Solly *et al.*, 2014; See *et al.*, 2019; but *see* Sun *et al.*, 2018). The monomeric composition of lignin further influences its biodegradability. For example, compared with other lignin types, higher proportions

© 2022 The Authors
New Phytologist © 2022 New Phytologist Foundation.
This is an open access article under the terms of the Creative Commons Attribution-NonCommercial License, which permits use, distribution and reproduction in any medium, provided the original work is properly cited and is not used for commercial purposes.

of G-type units can hinder lignin decomposition by facilitating carbon–carbon linkages that are less prone to decay (Goñi *et al.*, 1993; Talbot *et al.*, 2012). Thus, root decomposition is a function of both quantity and composition of lignin. In summary, the characterization of lignin abundance and composition in fine roots is essential to understanding root functions as well as root decomposition that affects the fate of root-derived carbon in soil.

Despite modern advances in plant tissue analysis, characterizing lignin in fine roots remains challenging. Although lignin has frequently been used as a proxy for litter quality (decomposition propensity) in biogeochemical models, no consensus has been reached on a standard method for lignin quantification. Lignin abundance is estimated using various methods that measure different aspects of lignin (Table 1). Without an understanding of how comparable these methods are, it is difficult to interpret and synthesize lignin data across studies and plant species. This problem is particularly acute in root studies, due to a lack of comparative studies and the limited number of species that have been studied.

A form of lignin quantification that is widely adopted across ecological studies relies on a two-stage sulfuric acid hydrolysis to separate extract-free tissue into an acid-soluble fraction and an acid-insoluble fraction (AIF). The AIF is operationally defined as lignin (i.e. AIF-defined lignin, or Klason lignin) and determined gravimetrically. This proximate estimate of lignin abundance has been routinely used in ecological studies for decades and provided the basis for the current notion that lignin negatively affects leaf and root decomposition (Taylor *et al.*, 1989; See *et al.*, 2019). However, compared with the wood tissues for which AIF analysis was originally designed (Sluiter *et al.*, 2010), fine roots comare often more chemically heterogeneous and may contain large amounts of nonlignin AIF components (e.g. suberin, tannin–protein complexes, Preston *et al.*, 2009; fungal tissues, Jurak *et al.*, 2015). Therefore, the AIF-defined lignin content in fine roots could be significantly interfered with by non-lignin AIF materials.

Comparing AIF analysis to lignin-specific techniques that estimate lignin by specifically quantifying lignin monomers will provide insight into how to interpret lignin data probed by the proximate AIF analysis. More lignin-specific methods have been used in root studies to measure lignin abundance and composition (e.g. Wang *et al.*, 2015, cupric oxide (CuO) oxidation; Leuschner *et al.*, 2003, thioacidolysis). Both CuO oxidation and thioacidolysis depolymerize lignin into well-defined diagnostic phenolic monomers (Hedges & Ertel, 1982, Rolando *et al.*, 1992), which are separated using chromatographic techniques and characterized using mass spectrometry. These methods quantify lignin content by measuring the abundance of diagnostic lignin compounds, and they are hence specific to lignin, although there is a potential for the underestimation of lignin due to incomplete depolymerization. Although CuO oxidation and thioacidolysis are both lignin-specific, depending on the plant species, their estimates of lignin properties may vary from each other as they cleave different inter-unit linkages. Thioacidolysis may underrepresent G-type lignin as it mainly cleaves β-O-4 linkages but leaves intact the additional carbon–carbon and ether linkages formed by the free C-5 position in G-type lignin (Ralph *et al.*, 2004; Del Río *et al.*, 2009). By contrast, CuO oxidation of lignin polymers is less specific (Dean, 1997). So far, little is known about how lignin content estimated by the proximate AIF analysis is related to that obtained by lignin-specific methods in fine roots across tree species, or how lignin-specific methods compare to each other. Elucidating such relationships is key to improving our understanding of the chemical components that influence root decomposition at a mechanistic level, as well to integrating root lignin data across studies for large-scale synthesis and modeling.

Another challenge for the routine estimation of root lignin is that these methods are time-consuming, labor-intensive, and hence are unsuitable for analyzing large-scale root samples, making lignin data less frequently collected than other root trait data. Although both nitrogen and lignin regulate root decomposition, in the global Fine-Root Ecology Database (FRED, Iversen *et al.*, 2017), observations of lignin are *c.* 90% lower than those of tissue nitrogen. These lignin records were largely based on proximate analysis and were limited to a restricted number of species. This lack of information is problematic, considering strong phylogenetic signals have been detected for other root traits when extended lineages of species have been studied (Valverde-Barrantes *et al.*, 2015). To our knowledge, few studies have compared lignin properties across a representative number of seed plant lineages. Reliable, yet high-throughput, techniques for assessing lignin content in fine roots may facilitate the collection of large-scale data for a better characterization of lignin in plant roots.

Methods that require less sample preparation, such as pyrolysis–gas chromatography–mass spectrometry (py-GC-MS) and Fourier transform infrared spectroscopy (FTIR), have been used to characterize lignin properties for wood and forage tissues (e.g. Ralph & Hatfield, 1991; Müller *et al.*, 2009) and may potentially be a useful tool for rapid characterization of lignin in fine roots. Pyrolysis (thermal decomposition under inert atmosphere) of plant biomass produces a large number of products from which lignin monomeric substructures and abundance can be inferred (Ralph & Hatfield, 1991; Del Río *et al.*, 2009). However, absolute lignin quantification by py-GC-MS is challenging because it is impractical to obtain individual response factors for the complex lignin-derived products (often > 40 compounds, Del Río *et al.*, 2012). Pyrolysis–gas chromatography–mass spectrometry is also less specific to lignin than CuO oxidation and thioacidolysis, as it does not distinguish between lignin and cell-wall bound hydroxycinnamates (van Erven *et al.*, 2018). Recently, van Erven *et al.* (2018) used py-GC-MS and an external reference with known lignin content to quantify the lignin abundance in wheat straw to an adequate degree of accuracy. Alternatively, pyrogram features obtained by py-GC-MS have been used to develop quantitative models to predict lignin content (e.g. Kleen *et al.*, 1993; Fahmi *et al.*, 2007). Fourier transform infrared spectroscopy is another rapid method of chemical analysis; it measures infrared spectra, features of which can be explained by various molecular vibrations (Smith, 2011). Modern FTIR coupled with attenuated total reflectance (ATR) removes the need for sample preparation with potassium bromide required in transmission FTIR, making it one of the fastest tools for chemical analysis. The IR band at 1510 cm^{-1} is characteristic

© 2022 The Authors
New Phytologist © 2022 New Phytologist Foundation.

Table 1 Overview of five analytical methods for characterizing lignin properties in plant tissues.

Lignin analysis	Lignin specificity	Method mechanisms	Potential disadvantages	Labor intensity	Hazardous reagents	Estimate of lignin abundance	Estimate of lignin composition
Two-stage sulfuric acid hydrolysis (i.e. Kalson lignin analysis and variants)	Low	A two-stage sulfuric acid hydrolysis was used to separate extract-free tissue into acid-soluble and acid-insoluble fractions (AIF)[1]. The AIF is used as an approximation of lignin (i.e. AIF-defined lignin) and is determined gravimetrically	AIF analysis is not specific to lignin because it measures an AIF that may include lignin and nonlignin materials (e.g. suberin, tannin–protein complexes, fungi cell walls)[2,3] that resist hydrolysis	*****	Concentrated sulfuric acid	✓	
CuO reaction	High	Mild oxidation by CuO was used to depolymerize lignin and release diagnostic phenolic monomers[4]. The monomers released can be quantified using chromatography mass spectrometry techniques	The recovery of lignin monomers may be low due to incomplete depolymerization of lignin and the overoxidation of lignin products[5]	*****	Organic solvents	✓	✓
Thioacidolysis	High	Thioacidolysis selectively cleaves β-O-4 linkages in uncondensed aryl ether structures of lignin[6]. This process releases well-defined diagnostic phenolic monomers that can be quantified by chromatography mass spectrometry techniques	Thioacidolysis mainly cleaves β-O-4 linkages (often the dominant linkage in angiosperms[7]) and thus may notably underestimate the amounts of G-type lignin by leaving intact the linkages formed by the free C-5 position that is unique to G-type lignin. Quantifying dimers after desulfurization may improve this method's representativity of lignin in plant tissues[8]	****	• Boron trifluoride diethyl etherate • Organic solvents particularly dioxane	✓	✓
Py-GC-MS (high-throughput)	Moderate	Pyrolysis uses high temperature to decompose lignin polymers under an inert atmosphere and releases a large number of lignin-derived products[9]. The released compounds can be quantified using chromatography mass spectrometry techniques. Pyrogram features may also be used to construct quantitative models against reference lignin estimates to predict lignin content	py-GC-MS did not distinguish between lignin and hydroxycinnamates, which can form similar pyrolysis products (e.g. 4-vinylphenol and 4-vinylguaiacol)[10]. In addition, obtaining individual response factors for the pyrolysis products required for accurate quantification can be challenging	**	–	✓	✓

© 2022 The Authors
New Phytologist © 2022 New Phytologist Foundation.

Table 1 (Continued)

Lignin analysis	Lignin specificity	Method mechanisms	Potential disadvantages	Labor intensity	Hazardous reagents	Estimate of lignin abundance	Estimate of lignin composition
FTIR-ATR (high-throughput)	Low	FTIR-ATR measures the mid-infrared region (from 4000 cm^{-1} to 400 cm^{-1}) that contains information arising from molecular vibrations[11]. The abundance of lignin can be assessed either by measuring bands characteristic of functional groups in lignin, or by constructing quantitative models using FTIR spectra and reference lignin estimates	A higher degree of uncertainty in assigning IR-absorbance to specific molecules when present in a complex matrix makes IR a relatively less specific technique. Lignin characteristic bands (e.g. *c.* 1500 cm^{-1}) may heavily overlap with other bands that arise from nonlignin components[11]	*	–	✓	

References: 1. Sluiter *et al.* (2010); 2. Preston *et al.* (2009); 3. Jurak *et al.* (2015); 4. Hedges & Ertel (1982); 5. Faust *et al.* (2018); 6. Rolando *et al.* (1992); 7. Del Río *et al.* (2009); 8. Lapierre (1993); 9. Ralph & Hatfield (1991); 10. van Erven *et al.* (2018); 11. Smith (2011). Labor intensity is an approximate estimate of the degree of labor and time required in the sample preparation process and the operation of the instrumentation used in each method, ranging from low (*) to high (*****). CuO, cupric oxide; FTIR-ATR, Fourier transform infrared spectroscopy-attenuated total reflectance; Py-GC-MS, pyrolysis-gas chromatography-mass spectrometry.

of aromatic skeletal vibration, and its relative intensity against carbohydrate bands has been shown to correlate with lignin abundance (Rodrigues *et al.*, 1998; Pandey & Pitman, 2004; Horikawa *et al.*, 2019). A combination of FTIR-ATR and quantitative modeling also exhibited a high degree of accuracy in predicting lignin content (Fahey *et al.*, 2017). The py-GC-MS and FTIR-ATR studies cited here often investigated the lignocellulose matrix from wood materials and focused on intraspecific variations or a few tree species. Compared with wood materials, fine roots have a very different tissue construction and are more chemically heterogeneous. To our knowledge, the applicability of high-throughput methods to the prediction of lignin properties in fine roots across broad ranges of tree species, either through direct measurements or predictive modeling, has not been explored.

Here, we compared five lignin methods (AIF analysis, CuO oxidation, thioacidolysis, py-GC-MS, and FTIR-ATR) for estimating the natural variability of lignin abundance and monomeric composition in fine roots across 34 tree species spanning major angiosperm clades (Fig. 1a). The primary aim of the study was to assess the comparability of different methods and their suitability for characterizing root lignin across tree species. Our samples represent the variability of root traits found in plant communities across biomes and global climate gradients (Valverde-Barrantes *et al.*, 2015). We tested a set of hypotheses/predictions for the comparability of lignin analyses. Our main hypotheses are as follows. (1) The abundance of AIF-defined lignin is disconnected from the lignin conten estimated by lignin-specific techniques (CuO oxidation and thioacidolysis) in quantifying root lignin across a broad range of tree species. This is because the abundance and variation of AIF-defined lignin in fine roots could be driven largely by non-lignin AIF materials. Specifically, we predict that AIF-defined lignin content is systematically higher than that estimated using lignin-specific techniques, and that the variation in AIF-defined lignin content is unrelated to variation in estimates from lignin-specific techniques. (2) We predict that the estimates of lignin abundance and monomer composition obtained using lignin-specific methods are relatively comparable due to limited interference from non-lignin materials in these methods. Alternatively, (3) their estimates may vary from each other due to their different mechanisms of releasing lignin-derived compounds. Specifically, thioacidolysis may underestimate the abundance of G-type lignin and leading to higher S : G ratio estimates than CuO oxidation. We further examined the applicability of high-throughput techniques (py-GC-MS and FTIR-ATR), through both direct measurements and predictive modeling, to capture the variability of lignin abundance and composition in fine roots across tree species.

Materials and Methods

Root sampling

We sampled roots from 34 trees species in two tree collections: The Holden Arboretum, Ohio (40°57′N and 82°28′W) and Boone County Arboretum, Kentucky (38°57′N and 84°43′W), during mid-summer (July–August) of 2010 and 2011, as described in a previous study (Valverde-Barrantes *et al.*, 2015). Samples from each species were taken from two adult trees within

© 2022 The Authors
New Phytologist © 2022 New Phytologist Foundation.

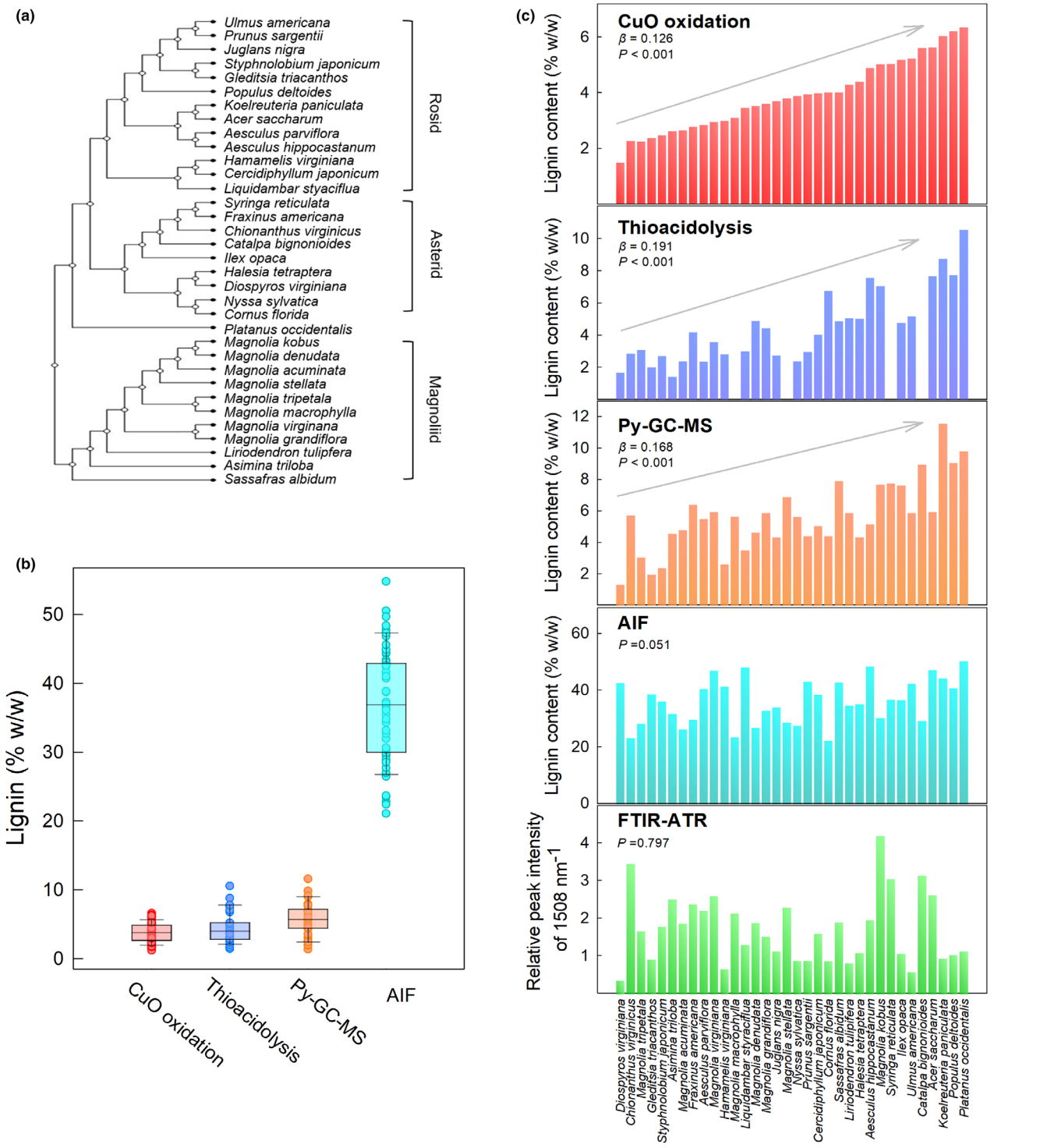

Fig. 1 Comparison of five analytical methods for estimating lignin abundance in fine roots (i.e. the most distal two orders of roots) across 34 angiosperm tree species. (a) List of the tree species with their phylogenetic relationships extracted from a molecular phylogeny in Zanne *et al*. (2014). The life history of these species and their representation in angiosperm super-orders are shown in Valverde-Barrantes *et al*. (2015). (b) Distribution of lignin content obtained using relatively lignin-specific methods (i.e. cupric oxide (CuO) oxidation, thioacidolysis, pyrolysis–gas chromatography–mass spectrometry (py-GC-MS), calibrated using a milled-wood lignin standard) and proximate acid-insoluble fraction (AIF) analysis. The box plots show the median (horizontal line), the interquartile range (box), and the whiskers (extending to the 5th and 95th percentiles, respectively), with individual biologically distinct root samples shown as circles. (c) Comparison of five methods of describing the variation in lignin abundance. To compare across methods, the tree species in five methods are ranked in the same way: in ascending order of lignin abundance, as determined by the CuO oxidation method. Significant and positive linear trends along such an order of tree species were observed for all three compound-specific methods (CuO oxidation, thioacidolysis, and py-GC-MS) ($P < 0.001$) but were largely absent in AIF analysis and Fourier transform infrared spectroscopy coupled with attenuated total reflectance (FTIR-ATR). The data for each species shown in (c) were obtained from the same biological root sample but by different methods (Supporting Information Table S1).

© 2022 The Authors
New Phytologist © 2022 New Phytologist Foundation.

a study site, with most of the species replicated at both sites (Table S1). Roots were identified by tracing back to the main stem, and a distal root segment was collected and preserved in 45 : 5 : 50, water : acetic acid : formalin as a reference. Root samples for further analysis were collected from two soil cores (10 cm diameter × 15 cm deep) within 2 m of the main stem and were transported to the laboratory with ice. Roots were separated from soil by soaking in water for 12 h and washing with deionized water to minimize soil contamination. The cleaned roots were compared to the reference for identification and were separated into different orders according to the method described by McCormack *et al.* (2015). The distal two orders of roots (i.e. fine roots), which are predominantly responsible for nutrient acquisition and root turnover (McCormack *et al.*, 2015), were included for chemical analysis. Roots were oven-dried at 65°C for 48 h and ground using a GenoGrinder (Spex SamplePrep, Metuchen, NJ, USA) at 500 rpm for 1 min. Due to sample limitation, AIF analysis and CuO oxidation were performed for all 64 biologically different samples, while subsets of these samples were performed for other methods (Table S1).

Acid-insoluble fraction analysis

The AIF analysis was conducted following the Klason protocol described in Ryan *et al.* (1990); this has been documented in a previous article (Valverde-Barrantes *et al.*, 2015). Briefly, polar and nonpolar extractives were removed by extractions of root samples with methanol (50%, 3×) followed by two extractions with dichloromethane. The extract-free residue was separated into an acid-soluble fraction and an AIF through a two-stage hydrolysis, first in 72% sulfuric acid (H_2SO_4) at 30°C for 1 h, followed by 2.5% H_2SO_4 with autoclaving at 121°C for 2 h. The AIF content was corrected for ash content after incineration of the AIF at 500°C for 4 h.

Isolation of the lignin standard for lignin-specific methods

The milled-wood lignin was prepared as described previously by Bjorkman (1956). Air-dried *Liriodendron tulipifera* sapwood was milled in a Wiley mill to pass 40 mesh and then extracted with 90% (v/v) acetone and ethanol : benzene (2 : 1, v/v). The extract-free wood was ball milled in a high-speed vibrating ball mill (MSK-SFM-3, MTI Corp., Richmond, CA, USA) under an N_2 environment with *c.* 70 ***g*** of force and a net milling time of 3 h. For every 2 min of milling a pause of 5 min was used to prevent overheating. The milled wood was extracted with dioxane (96%, v/v) for 24 h twice under mechanical stirring. The extracts were dried in a rotary evaporator followed by a N_2 evaporator to yield crude lignin isolates. The crude lignin was purified with 90% (v/v) acetic acid and 1,2-dichloroethane : ethanol (2 : 1, v/v) to obtain purified lignin isolates. The isolated lignin shows a high degree of purity (91.2 ± 0.6% in duplicates, Klason lignin) and was used as a lignin standard for lignin quantification via CuO oxidation, thioacidolysis, and py-GC-MS, to calibrate for the potentially incomplete depolymerization and loss of lignin-derived products.

Cupric oxide oxidation

The CuO oxidation procedure was according to Hedges & Ertel (1982) with modifications. Samples with a mass of *c.* 40 mg were extracted with methanol under sonication. Then, cell wall-bound phenols were removed using mild-base hydrolysis with 1 N NaOH at 85°C for 1 h. The remaining residue was dried and incubated in acid digestion vessels (model 4749; Parr Instrument Co., Moline, IL, USA) with CuO and $Fe(NH_4)_2(SO_4)_2.6H_2O$ in N_2-sparged 2 M NaOH at 155°C for 160 min. After incubation, samples were spiked with cinnamic acid and ethyl-vanillin (10 μg ml^{-1}) as internal standards. The released lignin phenols plus internal standards were extracted with pre-cooled ethyl acetate after the pH was adjusted to < 2. The extracted compounds were derivatized with N-methyl-N-(trimethylsilyl)-trifluoroacetamide with 1% trimethylchlorosilane (MSTFA +1% TMCS) and injected using 10 : 1 split ratio at 1 μl into GC-MS (7890 system and 5975C mass detector; Agilent, Santa Clara, CA, USA) with the injection port maintained at 270°C. The phenolic compounds were separated on a DB5-MS column (30 m × 250 μm × 0.25 μm; J&W Scientific, Folson, CA, USA), with the oven temperature starting at 70°C for 2 min followed by a ramp at 10°C min^{-1} to 270°C. Electron ionization was used, with an ionization energy of 70 eV. The source and quadrupole of the mass spectrometer were maintained at 250°C and 150°C, respectively, with the electron multiplier at a constant gain of 2 and the scanning range of the quadrupole at 50–600 amu. The same mass spectrometer parameters were used for thioacidolysis and py-GC-MS, unless otherwise stated. Twelve lignin-derived monomers were identified and quantified based on retention time, mass spectra and detector response of authentic standards (Table S2). Lignin content (% w/w) was estimated based on a standard curve of inputs of purified lignin vs their total yields of lignin phenols.

Thioacidolysis

Before thioacidolysis, *c.* 5 mg samples were extracted with methanol under sonication. The extract-free mass was incubated with 1 ml of N_2-purged thioacidolysis reagent consisting of 2.8% (v/v) boron trifluoride diethyl etherate (> 47.5% BF_3, Sigma-Aldrich), 10% (v/v) ethanethiol (97%, Sigma-Aldrich), 87.2% dioxane (v/v, Sigma-Aldrich), and bisphenol-E (internal standard, Sigma-Aldrich) at 100°C for 4 h. After incubation and cooling, 500 μl of product mixture was transferred to a glass tube, neutralized with 1 M sodium bicarbonate and acidified to pH < 2. One milliliter of water and 500 μl of pre-cooled ethyl acetate were added to the tube, vortexed, and left to sit for 10 min for phase separation. A 50 μl quantity of ethyl acetate phase was transferred to a GC vial and dried under vacuum. Next, 10 μl pyridine and 50 μl MSTFA +1% TMCS were added for silylation at 50°C for 40 min. One microliter of derivatized sample was injected at a 5 : 1 split ratio into GC-MS. The separation of thioacidolysis products was attained using a DB5-MS column. The column temperature was as follows: initial temperature, 80°C, ramped at 30°C min^{-1} to 200°C (for 2 min), and then ramped at 10°C min^{-1} to 300°C (for 10 min). The data were

© 2022 The Authors
New Phytologist © 2022 New Phytologist Foundation.

acquired in selective ion monitoring mode for syringyl monomers (299 *m/z*), coniferyl monomers (269 *m/z*), coumaryl monomers (239 *m/z*), and bisphenol-E (343 *m/z*). The lignin-derived monomers were quantified using the respective response factors relative to bisphenol-E (Harman-Ware *et al.*, 2016). Lignin content (% w/w) was determined based on a standard curve of inputs of purified lignin vs their total yields of lignin monomers.

Pyrolysis–gas chromatography–mass spectrometry

A 5150 pyroprobe (CDS Analytical, Oxford, PA, USA) directly coupled to the GC-MS was used to conduct the py-GC-MS. Approximately 2 mg of each sample was introduced into the pyroprobe in the quartz tube and supported by packed quartz wool (Ghetti *et al.*, 1996). The sample mass was determined based on preliminary studies to obtain reproducible results across species. The pyrolysis was performed at 500°C for 1 min. Helium was used to carry the pyrolysis products to the GC-MS, with an interface temperature of 300°C. Pyrolysis products were introduced at a split ratio of 200 : 1 into the GC-MS. The pyrolysis products were separated using a DB5-MS column, with the oven temperature starting at 80°C for 2 min and ramping at 8°C min^{-1} to 300°C (for 7 min). Forty-one pyrolysis products were identified by comparing retention time and mass spectra against the signature fragments of lignin pyrolysis products published by van Erven *et al.* (2017) and confirmed using the NIST-Mass Spectral library (2017; Table S3). We quantified lignin content as per van Erven *et al.* (2018). Specifically, the peak area of a lignin-derived product was divided by its relative response factors (RRFs) and multiplied by its molecular weight. Lignin content was then determined based on the total corrected area of lignin-derived products of each sample and that of the purified lignin as follows:

$$\text{Lignin content}\ (\%) = \frac{\sum_{i=1}^{38} \frac{A_{i,\text{sample}}}{\text{RRF}_i} \times M_i \times m_{\text{lignin}}}{\sum_{i=1}^{38} \frac{A_{i,\text{lignin}}}{\text{RRF}_i} \times M_i \times m_{\text{sample}}} \times 100\%$$

where i refers to the compound number, A is the peak area, M is the molecular weight, and m is the dry weight of the samples or purified lignin. Since we used the RRFs published by van Erven *et al.* (2017) and because py-GC-MS is less specific to lignin compared with CuO oxidation and thioacidolysis, we considered this method to be 'semi-quantitative' and further used pyrogram-based multivariate modeling to predict lignin abundance. More accurate quantification of lignin could be achieved using ^{13}C-labeled lignin as an internal standard (van Erven *et al.*, 2018).

Fourier transform infrared spectroscopy–attenuated total reflectance

The FTIR spectrum was collected with a Thermo Scientific Nicolet iS50 FT-IR Spectrometer (Thermo Fisher, Waltham, MA, USA) using a diamond single reflection ATR accessory. Sixty scans at a resolution of 4 cm^{-1} were recorded. A blank spectrum of air was taken as a background measure before each sample and was subtracted from the sample spectrum. The spectra were corrected using advanced ATR correction followed by rubber-band baseline correction (Baker *et al.*, 2014) in a consistent manner across all root samples using the OMNIC v.9.2 software package. Band heights were measured against the baseline to represent the intensity of the bands. The relative absorption intensity of the band at *c.* 1508 cm^{-1} (characteristic of aromatic skeletal vibration) to the intensity of the band at 1370 cm^{-1} (C–H deformation in polysaccharides, Pandey & Pitman, 2003), both of which were present across all samples, was used to approximate lignin abundance. We also used FTIR-spectrum based multivariate-modeling to predict lignin abundance.

Method performance

Two sets of additional quality control (QC) materials were used to examine the reproducibility of the lignin quantification methods. For this purpose, oven-dried (65°C, 48 h) and pulverized *Acer saccharum* leaf litter and roots (< 2 mm in diameter) were used to represent plant tissues with relatively low and high lignin content, respectively. The reproducibility of the lignin quantification methods was examined by replicate analyses of both QC materials on different days of analysis. High reproducibility was obtained for the lignin content (RSD: 2.16 to 7.85%) and S : G ratios (RSD: 2.28 to 6.68%) in QC materials across the CuO reaction, thioacidolysis, and py-GC-MS methods (Table S4). In addition, a subset of root samples was analyzed in duplicate for these compound-specific techniques, with RSD ranging from 0.05 to 9.35% (Table S4). The AIF analysis and FTIR-ATR were performed in duplicate for all samples and exhibited satisfactory reproducibility (RSD for AIF %: 6.54 ± 4.53%; RSD for relative intensity 1508 cm^{-1} in FTIR spectra: 4.62 ± 3.86%). To assess the overall accuracy of the protocols and calibration methods used in the lignin quantification, we additionally compared three inputs of purified lignin vs their estimated lignin mass by CuO reaction, thioacidolysis, and py-GC-MS, as external validation. The obtained slopes were close to 1 with high r^2 values (slope: 0.964 to 0.976; r^2: > 0.995, Table S4).

Data analysis

Data analysis was performed using the R software package (v.4.0.5). Pearson's correlation analysis was performed to investigate the pairwise relationships between estimates obtained using different methods and between predicted and observed values. One-way analysis of variance ANOVA was performed to determine whether phylogenetic clade had an effect on lignin composition, followed by Tukey's HSD test for pair-wise comparison. Data were log-transformed to improve the homogeneity of variance before being analyzed. We examined the relationships between root diameter and lignin abundance with piecewise models using the R software package SEGMENTED. The piecewise model assesses ecological thresholds by fitting two lines with different slopes that join together at a threshold point (Muggeo, 2008). For this model, the Davies' test was used to test the significant change of slope (i.e. the threshold of changes).

We used partial least squares regression (PLSR) and least absolute shrinkage and selection operator (LASSO) approaches to

© 2022 The Authors
New Phytologist © 2022 New Phytologist Foundation.

calibrate high-dimensional data obtained from high-throughput py-GC-MS and FTIR-ATR against lignin content and composition quantified by the lignin-specific CuO oxidation method. The PLSR approach has been used frequently to predict lignin content. However, PLSR is prone to overfitting and does not provide statistical significance for variables (Wold *et al.*, 2001). An alternative technique, LASSO, has gained popularity, as it often provides improvements over PLS-based models (Bujak *et al.*, 2016; Erler *et al.*, 2020) and is easier to interpret by selecting relevant features based on statistical significance (Bujak *et al.*, 2016). All 41 pyrogram features were combined into a predictor matrix for pyrolysis-based modeling. The FTIR-ATR spectra were used to construct the predictor matrix for FTIR-based modeling. We tested pre-processing algorithms for the FTIR-ATR spectra: first derivative, second derivative, and vector normalization. We used vector normalization for model fitting because this algorithm consistently produced better model performance than other algorithms. The predictor data were mean-centered and scaled before model construction. Samples were split into two groups, the first (80% of the total samples) being used for calibration and cross validation, and the second (20%) for prediction of external samples. The calibration models for PLSR were developed using the R package PLS and constructed with internal cross validation, where the model with the smallest root mean square error (RMSE) of n-fold cross validation was selected. For LASSO model calibration, we first used cross-validation (package GLMNET) to identify the optimum λ value that produced the lowest RMSE. The most parsimonious model chosen by cross-validation was then constructed using the function *glmnet*.

Results

Lignin abundance

Our data showed a broad range of variation in lignin abundance across tree species (Fig. 1). As expected by hypothesis 1, the more lignin-specific methods (CuO, thioacidolysis, and py-GC-MS) generally agree on a range of 2–10% by weight for the lignin content of fine roots across 34 phylogenetically diverse tree species, yet AIF analysis estimated an AIF-defined lignin content that was *c.* 5–10-fold higher, in the range of 21–50% (Fig. 1b). To compare the variability of lignin content estimated by different methods, the tree species in five methods were ranked in the same way, that is, following the ascending order of lignin content determined by CuO oxidation. Again, AIF-defined lignin content exhibited a very different pattern of variation from the results obtained using lignin-specific techniques (Fig. 1c). For example, three lignin-specific techniques agreed that the lignin content of *Diospyros virginiana* roots was among the lowest across 34 tree species; however, *D. virginiana* exhibited a high AIF-defined lignin content relative to other species. Consequentially, the AIF-defined lignin content had a weak correlation or no correlation with the findings of the lignin-specific methods (Table 2). The correlation between the AIF-defined lignin content and lignin content determined using lignin-specific methods was markedly higher within more closely related species. The correlation coefficients between AIF-defined lignin content and CuO reaction estimates increased from 0.298 ($P = 0.019$) across all species to 0.556 ($P = 0.005$) within the rosid lineage; the correlation between AIF-defined lignin content and thioacidolysis estimates increased from being insignificant across all species to 0.644 ($P = 0.024$) within rosids (Table 2).

Table 2 Pearson correlation matrix for lignin abundance of fine roots obtained from five analytic methods across 34 angiosperm tree species, and within the rosid clade.

	CuO	Thioacidolysis	Py-GC-MS	FTIR-ATR
Across all species				
Thioacidolysis	**0.876*** ** (32)			
Py-GC-MS	**0.780*** ** (37)	**0.738*** ** (30)		
FTIR-ATR	0.038 (53)	0.045 (32)	0.224 (34)	
AIF	**0.298* (64)**	0.340 (32)	0.144 (37)	**−0.328*** (53)
Within the rosid clade				
Thioacidolysis	**0.922*** ** (14)			
Py-GC-MS	**0.899*** ** (14)	**0.815**** (13)		
FTIR-ATR	0.088 (19)	0.185 (14)	−0.027 (13)	
AIF	**0.556**** (25)	**0.644*** (14)	0.323 (14)	−0.010 (19)

Asterisks denote significant Pearson correlations (two-tailed; *, $P < 0.05$; **, $P < 0.01$; ***, $P < 0.001$). Bold numbers denote significance at $P < 0.05$. Values are Pearson's correlation coefficients, with the sample sizes in parentheses. We note that only values obtained from the same biological root sample by different methods (see Table S1) were included in the pairwise comparison. AIF, acid-insoluble fraction analysis; CuO, cupric oxide reaction; FTIR-ATR, Fourier transform infrared spectroscopy-attenuated total reflectance; Py-GC-MS, pyrolysis-gas chromatography-mass spectrometry.

As expected by hypothesis 2, the methods that are highly specific to lignin (i.e. CuO oxidation and thioacidolysis), exhibited comparable distributions and similar patterns of variation in the lignin content of fine roots across tree species (Fig. 1b,c). The median estimates of lignin content across 34 tree species were similar for the CuO oxidation and thioacidolysis methods (3.74% vs 4.12% w/w). They also had the highest correlation coefficient ($r = 0.876$, $P < 0.001$, Table 2) among pairwise relationships across five lignin methods. In particular, these lignin-specific techniques consistently showed that fine roots of many magnoliids, such as *Magnolia tripetala*, *Asimina triloba*, and *Magnolia acuminata*, were the least lignified (Fig. 1c). Lignin content estimated using py-GC-MS also exhibited a significant and moderate correlation with those estimated using CuO oxidation and thioacidolysis (CuO oxidation, $r = 0.780$, $P < 0.001$; thioacidolysis, $r = 0.738$, $P < 0.001$, Fig. 1; Table 2), but in several species (e.g. *Chionanthus virginicus*) py-GC-MS estimated substantially higher lignin content than the other two methods.

The relative intensity of the lignin characteristic band observed using the FTIR-ATR exhibited a strikingly different pattern of variation across tree species from that observed using lignin-specific techniques (Fig. 1c). The intensity of this band did not correlate with the lignin content determined using lignin-specific techniques across all 34 species and within the rosid lineage (Table 2).

Using CuO oxidation for the same sample set, our previous study demonstrated that lignin had a negative two-phase

© 2022 The Authors
New Phytologist © 2022 New Phytologist Foundation.

relationship with root diameter (Xia *et al.*, 2021). Next, we tested whether this interspecific organization of lignin would be captured by AIF-defined lignin. Lignin content obtained from both CuO oxidation and AIF analysis exhibited a general two-phase relationship with root diameter (Fig. 2). However, the relationship was stronger for CuO oxidation (CuO oxidation: $r^2 = 0.363$, $P < 0.001$; AIF: $r^2 = 0.212$, $P < 0.001$), and the threshold of the two-phase relationship was not significant for AIF analysis (David's test, $P = 0.186$, Fig. 2).

Lignin monomer composition

The S : G ratios estimated by CuO oxidation and thioacidolysis exhibited similar patterns of variation across tree species and were highly correlated with each other ($r = 0.921$, $P < 0.001$, Fig. 3; Table 3). Although thioacidolysis is expected to underestimate G-type lignin and thus produce higher S : G ratios than CuO oxidation (hypothesis 3), the S : G ratios obtained via the CuO oxidation and thioacidolysis methods exhibit a strong linear relationship, with a slope close to 1 ($P < 0.001$, Fig. 4). The S : G ratios obtained using the py-GC-MS method exhibited moderate correlations with those obtained by CuO oxidation ($r = 0.668$, $P < 0.001$) and thioacidolysis ($r = 0.614$, $P < 0.001$, Fig. 3; Table 3). The CuO oxidation, thioacidolysis and pyrolysis methods demonstrated similar distributions of S : G ratios across three angiosperm lineages and were all able to distinguish the fundamental differences in lignin monomeric composition among different phylogenetic clades, where rosids tended to grow roots with lower S : G ratios than asterids (Fig. 3).

Two Asterids, *Catalpa bignonioides* and *C. virginicus*, showed substantially lower S : G ratios for py-GC-MS than for other lignin methods (Figs 3, 4). Consequently, correlations between py-GC-MS and other methods improved when only rosids were included (CuO: $r = 0.824$, $P < 0.001$; thioacidolysis: $r = 0.742$, $P = 0.004$, Table 2). The lower S : G ratios in these two asterids were largely driven by 4-vinylguaiacol, which may originate from hydroxycinnamates. This moiety accounted for 81.0% and 60.5% (w/w) of total G-type pyrolysis products in *C. bignonioides* and *C. virginicus*, respectively, compared with an average of 40.7 ± 7.0% for the rest of the species (Fig. S1). Similarly, these two species also exhibited a strikingly high relative abundance of 4-vinylphenol relative to other species (Fig. S1). These observations suggest interference from hydroxycinnamates in the estimates of lignin composition by py-GC-MS.

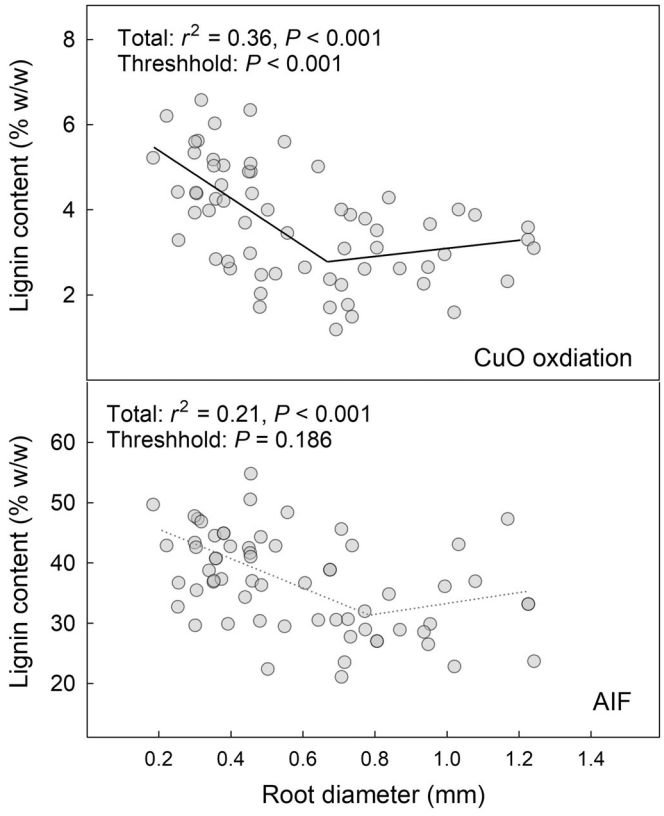

Fig. 2 Piecewise relationships between root diameter and lignin abundance measured by cupric oxide (CuO) reaction and the proximate acid-insoluble fraction (AIF) analysis.

Predictive models based on high-throughput techniques

The py-GC-MS-based models predicted lignin content and composition with a high degree of accuracy (Fig. 5; Table 4). For lignin abundance, the r^2 and RMSE values of the PLSR calibration model were 0.906 and 0.370, respectively; the r^2 and RMSE values of the external validation were 0.958 and 0.271. Partial least squares regression also showed good predictions for lignin monomeric composition (calibration: $r^2 = 0.952$; RMSE = 0.094; prediction: $r^2 = 0.932$; RMSE = 0.101). The LASSO models yielded slightly lower fittings than PLSR and exhibited lower r^2 and higher RMSE values in calibration models and external validation for both lignin content and composition (Fig. S2). However, LASSO provided chemically meaningful information about the source of predictability (Tables S5, S6). The LASSO model selected five characteristic S-type pyrogram features with positive coefficients and five G-type features with negative coefficients to predict S : G ratios (Table S6). Among pyrolysis products, 4-vinylphenol is negatively related to lignin content and 4-vinylguaiacol-although a major G-type product-was not selected by LASSO as a predictor for the S : G ratio, further supporting the idea that these moieties contribute to the discrepancy between py-GC-MS and CuO reaction.

When coupled with modeling, FTIR-ATR spectra demonstrated moderate prediction power to predict root lignin content (Figs 5, S2; Table 4). The r^2 and RMSE values of the FTIR-based PLSR calibration model were 0.758 and 0.590 respectively; the r^2 and RMSE values of the external validation were 0.797 and 0.694. The FTIR-based LASSO model revealed key wavelength-clusters for predicting lignin abundance (Table S7). Although a characteristic band at *c.* 1500 cm^{-1} often indicates the presence of lignin, LASSO did not include this band in its selection of lignin predictors. Rather, the wavelength clusters around 1125 nm^{-1} (C–H stretch potentially from guaiacyl and syringyl) and 1274 nm^{-1} (C–O of guaiacyl ring stretch, guaiacyl ring breathing) were positively related to lignin content. The wavenumber clusters around 906 cm^{-1} (C–H deformation in carbohydrates) and 1432 cm^{-1}

© 2022 The Authors
New Phytologist © 2022 New Phytologist Foundation.

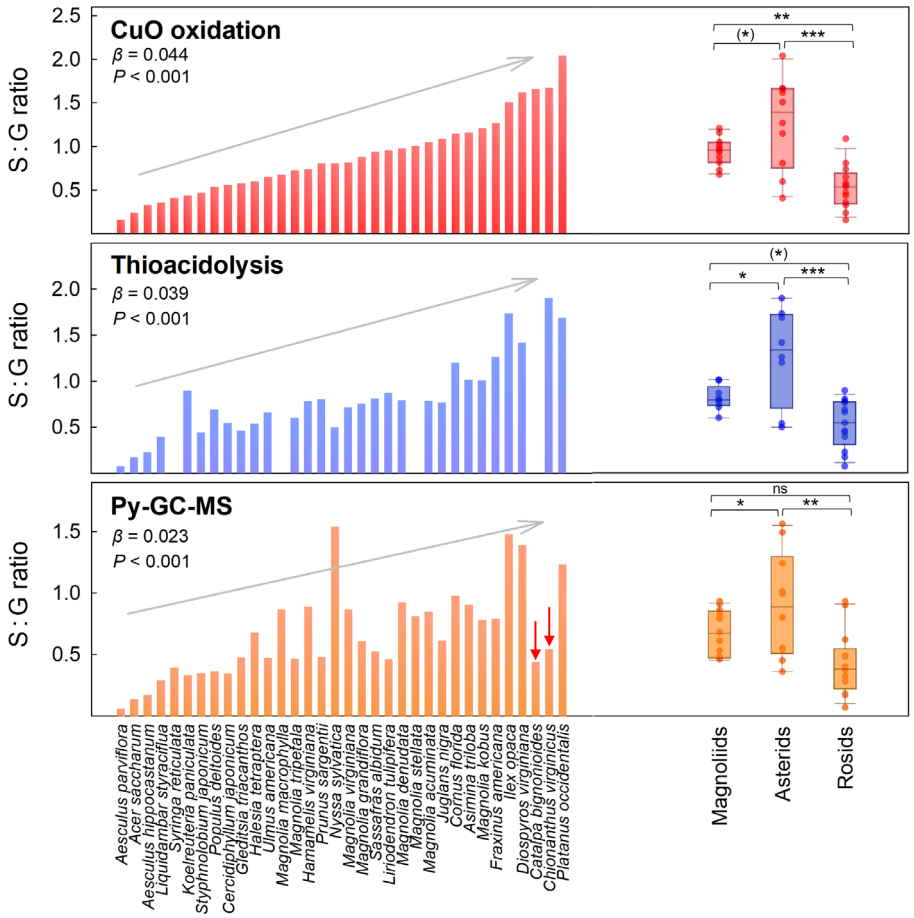

Fig. 3 Comparison of three analytical methods for measuring lignin monomeric composition in fine roots (i.e. the most distal two orders of roots) across 34 angiosperm tree species. To compare across the different methods, the tree species are ranked in the same way: in ascending order of the ratio of syringyl and guaiacyl units (the S : G ratio), as determined by the cupric oxide (CuO) oxidation method. Significant and positive linear trends along such an order of tree species were observed for all three methods. The box plots show the distribution of S : G ratios in fine roots from the tree species grouped to three major angiosperm lineages (magnoliids, asterids, and rosids). The median (horizontal line), the interquartile range (box), the whiskers (extending to the 5th and 95th percentiles, respectively), and individual biologically distinct root samples (circles) are shown in the box plots. Asterisks indicate significant differences ((*), $P < 0.1$; *, $P < 0.05$; **, $P < 0.01$; ***, $P < 0.001$; ns, not significant). The red arrows highlight the two asterids *Catalpa bignonioides* and *Chionanthus virginicus*, which showed considerably lower S : G ratios by pyrolysis–gas chromatography–mass spectrometry (py-GC-MS) compared to those obtained using the other two methods.

Table 3 Pearson correlation matrix for the ratio of syringyl and vanillyl units in lignin polymer of fine roots obtained from three analytic methods across 34 angiosperm tree species and that within the rosid clade.

	CuO	Thioacidolysis
Across all species		
Thioacidolysis	**0.921***** (32)	
Py-GC-MS	**0.668***** (37)	**0.614***** (30)
Within the rosid clade		
Thioacidolysis	**0.773***** (14)	
Py-GC-MS	**0.824***** (14)	**0.742**** (13)

Asterisks denote significant correlations (**, $P < 0.01$; ***, $P < 0.001$). Bold numbers denote significance at $P < 0.05$. Values are Pearson's correlation coefficients, with the sample sizes in parentheses. CuO, cupric oxide reaction; Py-GC-MS, pyrolysis-gas chromatography-mass spectrometry.

(symmetric CH_2 bending in cellulose) were negatively related to lignin content and may be indicators of carbohydrates. The FTIR spectra coupled with modeling was unable to accurately predict lignin composition and exhibited lower r^2 and higher RMSE in calibration models than py-GC-MS-based models (Figs 5, S2; Table 4). In the external validation, the predictions of S : G ratios from FTIR-based models did not correlate significantly with the observed S : G ratios.

Discussion

Because of its heteropolymeric nature, lignin in plants has been analyzed using different methods, either proximate or lignin-specific, across ecological studies. Here, we compared five analytical methods for measuring lignin abundance and monomeric composition in fine roots across phylogenetically diverse tree species and evaluated the comparability and suitability of methods of lignin characterization (Table 5). Although AIF-defined lignin has conventionally been used to indicate root chemistry and related to root decomposition, the content of AIF-defined lignin in fine roots was disconnected from the lignin content estimated by lignin-specific techniques (Fig. 1; Table 2). Compared with lignin-specific techniques, AIF-defined lignin content was systematically higher and the variability of AIF-defined lignin across tree species was largely unrelated to that described using lignin-specific techniques. In addition, AIF analysis appears to be less sensitive to capturing biologically meaningful patterns of root lignin (e.g. the relationship between lignin and root diameter, Fig. 3).

In comparison with wood tissues, for which AIF analysis was originally designed, fine roots are more chemically complex and can accumulate large amounts of non-lignin compounds (e.g. condensed tannins, proteins, suberins) that also contribute to the acid-insoluble fraction of root tissues (Preston *et al.*, 2009; Suseela & Tharayil, 2018). Mycorrhizal fungi that frequently form

© 2022 The Authors
New Phytologist © 2022 New Phytologist Foundation.

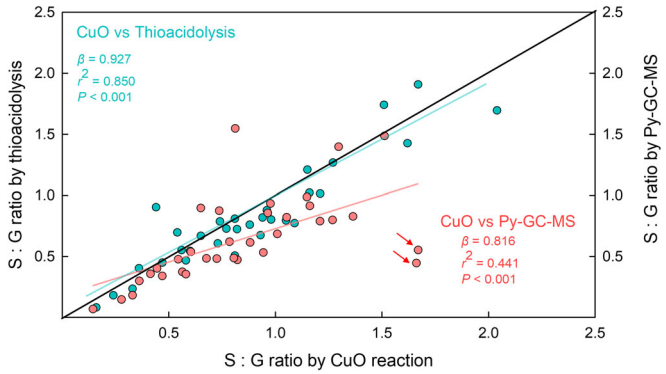

Fig. 4 The relationship of the ratio of syringyl and guaiacyl (the S : G ratio) characterized by three compound-specific analytical methods (cupric oxide (CuO) oxidation, thioacidolysis, and pyrolysis–gas chromatography–mass spectrometry (py-GC-MS)). The one-to-one line is shown as a solid black line. The slopes (β) and *P*-values are shown for each pairwise relationship (i.e. CuO vs thioacidolysis and CuO vs py-GC-MS). The red arrows highlight the two asterids *Catalpa bignonioides* and *Chionanthus virginicus*, which showed considerably lower S : G ratios by py-GC-MS when compared with those obtained using the other two methods.

symbioses with fine roots may further interfere with AIF analysis. This is because mycorrhizal fungi could account for a significant proportion of mycorrhizal root biomass (up to 10%, Ekblad *et al.*, 1995) and fungal biomass was shown to be efficiently preserved in the acid-insoluble fraction (Jurak *et al.*, 2015). Condensed tannins, suberins, and mycorrhizal fungal mass are not only abundant in fine roots but are also responsive to environmental conditions (Simard *et al.*, 2012; Suseela & Tharayil, 2018). Large amounts of, and high variability of, nonlignin AIF materials in root tissues limit the ability of AIF analysis to appropriately isolate root lignin and assess its quantity and variation. Significant nonlignin ATF materials in fine roots may explain why fine roots, which are often less lignified according to root anatomy (Guo *et al.*, 2008), frequently exhibited higher quantities of AIF-defined lignin (in a range of 25% to > 50%, w/w) than wood biomass, which was found to have lignin content in the range of 10–30% (Fig. 6). Lignin-specific techniques in this study agree on 2–10% (w/w) for lignin content in fine roots across a broad range of tree species, which is more closely in line with previous observations that fine/absorptive roots often show a large cortex with limited lignification and a lack of heavily lignified secondary tissues (Soukup *et al.*, 2004; McCormack *et al.*, 2015). The disconnection between AIF analysis and lignin-specific methods suggests that AIF-defined lignin in fine roots should be interpreted differently from lignin as it measures very different components of root chemistry. As such, the widely observed negative effect of acid-insoluble fraction on root decomposition may not necessarily result from the recalcitrance of lignin but is a result of multiple components in root tissues that are generally resistant to degradation. Thus, AIF might corelate with rate of decomposition of tissue more than with any of its chemical constituents. We also advise that research synthesizing root traits in large-scale studies should carefully consider the lignin methods used because of the low comparability in terms of both absolute quantity and variation of root lignin between AIF analysis and other lignin methods.

Our finding that the correlations between the contents of AIF-defined lignin and those obtained from lignin-specific methods improved within more closely related species demonstrates the potential of AIF-defined lignin as a predictor for lignin content within closely related trees. Phylogeny has been shown to explain variations in root chemistry, where elemental concentrations, and carbohydrate and phenolic profiles in roots tend to be more similar within more closely related species (Valverde-Barrantes *et al.*, 2015; Senior *et al.*, 2016; Xia *et al.*, 2021). Therefore, closely related species may develop roots that are relatively similar in terms of chemical composition and thus similar in their matrix effects, leading to an improved correlation between the AIF-defined lignin content and the lignin polymer content.

More lignin-specific methods such as CuO oxidation, thioacidolysis and py-GC-MS exhibited fairly comparable estimates of lignin content and composition, in terms of both quantity and variation. Although thioacidolysis mainly cleaves β-O-4 linkages and is expected to underestimate G-type lignin, lignin content and S : G ratios estimated by CuO reaction and thioacidolysis were highly correlated and exhibited a linear relationship at a slope close to 1. The high degree of comparability between these two methods may be a result of the fact that β-O-4 linkages are a predominant bond type in lignin, accounting for 72–86% of the lignin linkages in angiosperm trees (Del Río *et al.*, 2009; Parthasarathi *et al.*, 2011; Talbot *et al.*, 2012). In comparison, the estimates of lignin content and composition obtained from py-GC-MS exhibited lower correlations with estimates from CuO oxidation and thioacidolysis. This discrepancy may partly arise as a result of the interference of cell-wall bound hydroxycinnamates in py-GC-MS. The substantially lower S : G ratios in *C. bignonioides* and *C. virginicus* and the higher lignin content in *C. virginicus* estimated by py-GC-MS were largely driven by the disproportionally high relative abundance of 4-vinylguaiacol and/or 4-vinylphenol moieties that can be formed from both lignin and hydroxycinnamates upon pyrolysis. Indeed, our previous study showed that *C. bignonioides* and *C. virginicus* roots were abundant in bound hydroxycinnamates (Xia *et al.*, 2021). They had the highest and the third highest bound ferulic acid content among all 34 species, and their bound hydroxycinnamate content was 20% and 28% of their lignin content (Xia *et al.*, 2021, see also Fig. S1). Additional steps, such as removing extractable and ester-linked hydroxycinnamates or conducting pyrolysis in the presence of tetramethylammonium hydroxide (Filley *et al.*, 2006), would increase the lignin specificity of py-GC-MS. Together, these findings demonstrate that the CuO reaction and thioacidolysis were fairly comparable in their estimates of lignin content and composition in fine roots of angiosperm trees, whereas the bound hydroxycinnamates that are often abundant in root tissues may significantly interfere with py-GC-MS characterization of lignin.

Although direct measurement in root samples by py-GC-MS may be interfered with by nonlignin materials, py-GC-MS combined with multivariate models predicted lignin abundance and composition with a high degree of accuracy. This highlights the feasibility of py-GC-MS as a fast-screening technique for quantifying lignin content and composition in fine roots across

© 2022 The Authors
New Phytologist © 2022 New Phytologist Foundation.

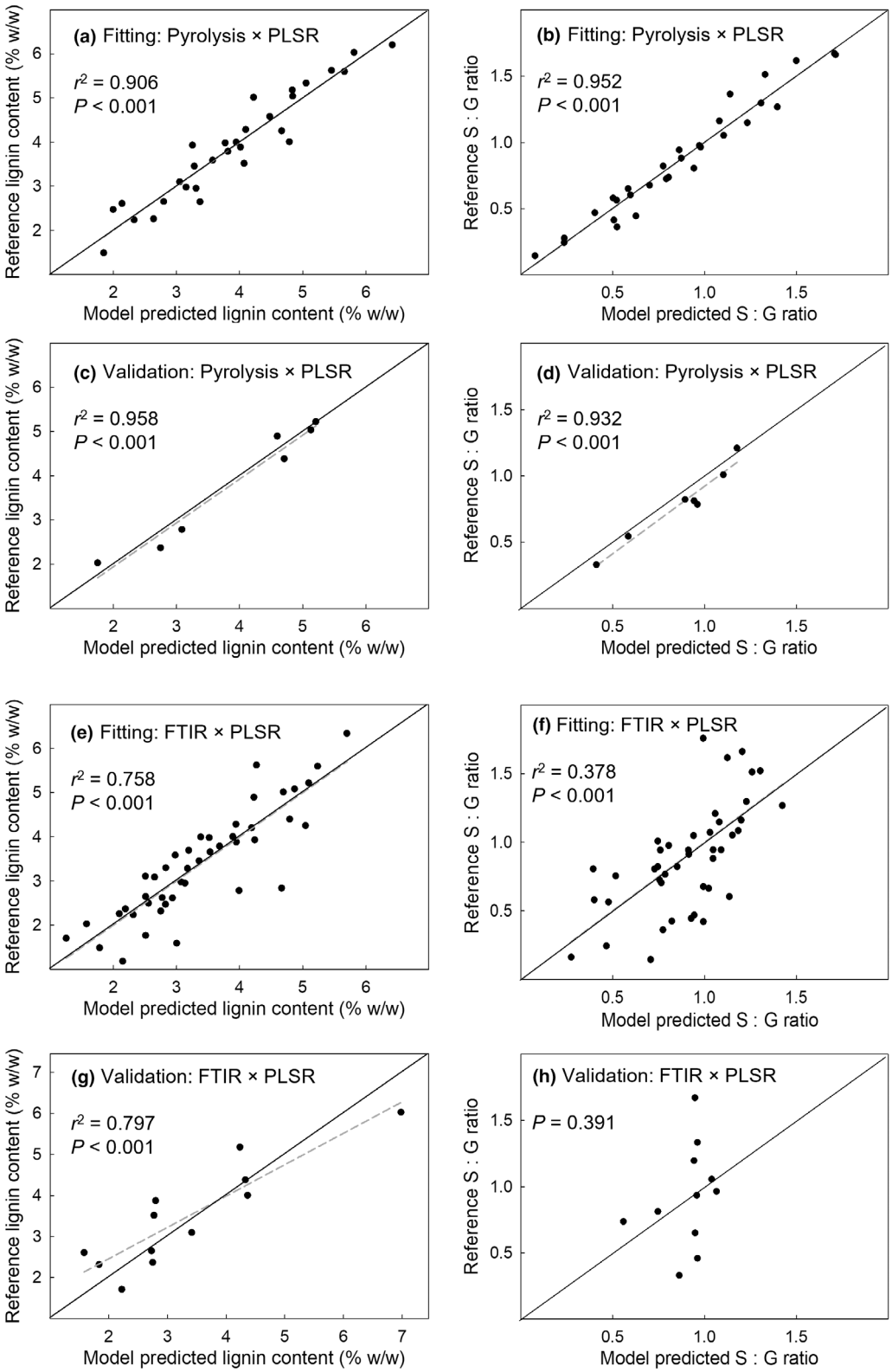

Fig. 5 Partial least square regression (PLSR) model fittings and external validations for the prediction of lignin content and monomeric composition in fine roots (i.e. the most distal two orders of roots) across tree species based on high-throughput techniques. The model fittings for lignin content and S : G ratios obtained using the pyrolysis–gas chromatography–mass spectrometry (py-GC-MS) method are shown in (a) and (b), respectively, with the corresponding external validations shown in (c, d). The model fittings for lignin content and S : G ratios based on Fourier transform infrared spectroscopy coupled with attenuated total reflectance (FTIR-ATR) are shown in (e) and (f), respectively, with the corresponding external validations shown in (g, h). The unity lines are shown as solid lines. The reference values of lignin abundance and monomeric composition were determined using cupric oxide (CuO) oxidation analysis, which is lignin-specific.

© 2022 The Authors
New Phytologist © 2022 New Phytologist Foundation.

	Py-GC-MS		FTIR-ATR	
	Abundance	Composition	Abundance	Composition
PLSR				
r^2	0.906	0.952	0.758	0.378
RMSE_CV	0.849	0.164	1.146	0.408
No. of PLSR factors	5	5	7	2
RMSE_calibration	0.370	0.094	0.590	0.332
RMSE_prediction	0.271	0.101	0.694	0.356
LASSO				
r^2	0.845	0.891	0.643	0.306
λ	0.084	0.045	0.095	0.116
DEV%	82.39	84.28	60.40	20.64
No. of predictors	11	11	17	5
RMSE_calibration	0.506	0.165	0.750	0.374
RMSE_prediction	0.402	0.162	0.608	0.412

DEV%, percent deviance explained by the model; RMSE, root mean square error.

Table 4 Performance of partial least squares regression (PLSR) and least absolute shrinkage and selection operator (LASSO) models for the prediction of lignin content and monomeric composition across tree species from high-throughput pyrolysis–gas chromatography–mass spectrometry (py-GC-MS) and Fourier transform infrared spectroscopy coupled with attenuated total reflectance (FTIR-ATR).

Table 5 Assessment of five analytical methods of characterizing lignin properties in fine roots across angiosperm tree species.

Lignin analytical method	Suitability of methods for different goals	Predictability for lignin via multivariate modeling
AIF analysis	• Compared with lignin-specific techniques, AIF analysis systematically overestimates lignin content by *c.* 5–10 fold and is not a good predictor of the variation in root lignin content across angiosperm tree species • AIF-defined lignin may be a good predictor of the variation in root lignin within more closely phylogenetically related trees • AIF% in root tissues should be interpreted separately from lignin content as it measures different aspects of root chemistry from lignin polymers	–
CuO reaction followed by GC-MS	• CuO and thioacidolysis are lignin-specific methods that are suitable for describing the variability of lignin abundance and composition in fine roots across angiosperm tree species	–
Thioacidolysis followed by GC-MS/SIM	• These two methods, although based on different mechanisms, highly correlate with each other in their measurements of lignin content and composition and are thus comparable in characterizing lignin in fine roots across angiosperm tree species • Because of the potentially incomplete polymerization and loss of lignin-derived products in these methods, use of lignin standards with natural interunit linkages as a reference is essential to obtaining more accurate lignin quantification • They are not suitable for large-scale experiments because they are labor-intensive and/or involve the use of hazardous reagents	
Py-GC-MS (high-throughput)	• Direct measurement of py-GC-MS is less lignin-specific and generates a moderate correlation with lignin-specific methods in its estimates of lignin abundance and composition in roots. Py-GC-MS of lignin may be significantly interfered with by cell-wall bound hydroxycinnamates that are often abundant in fine roots • It can accommodate experiments with relatively large samples and limited sample amounts. In this case, we recommend removing extractable and ester-bound hydroxycinnamates before pyrolysis or performing thermochemolysis in the presence of tetramethylammonium hydroxide to increases the specificity of pyrolysates. • When combined with quantitative modeling, it exhibited a high degree of prediction power for lignin content and composition, and thus may be a suitable tool for the large-scale screening of lignin properties in fine roots across tree species	• High for lignin content • High for lignin monomeric composition
FTIR-ATR (high-throughput)	• The lignin characteristic band (*c.* 1500 cm^{-1}) in IR spectra is not a good predictor of root lignin content across broad ranges of angiosperm tree species • When combined with predictive modeling, FTIR spectra showed moderate prediction power for lignin content, but were unable to predict lignin composition. We recommend the use of FTIR-ATR combined with modeling as a fast pre-screening tool for lignin abundance in fine roots when lignin composition is not of interest	• Moderate for lignin abundance • Unable to predict lignin monomeric composition

AIF, acid-insoluble fraction; CuO, cupric oxide; FTIR-ATR, Fourier transform infrared spectroscopy-attenuated total reflectance; GC-MS, gas chromatography-mass spectrometry; GC-MS/SIM, GC-MS in selective ion monitoring mood; Py-GC-MS, pyrolysis-GC-MS.

© 2022 The Authors
New Phytologist © 2022 New Phytologist Foundation.

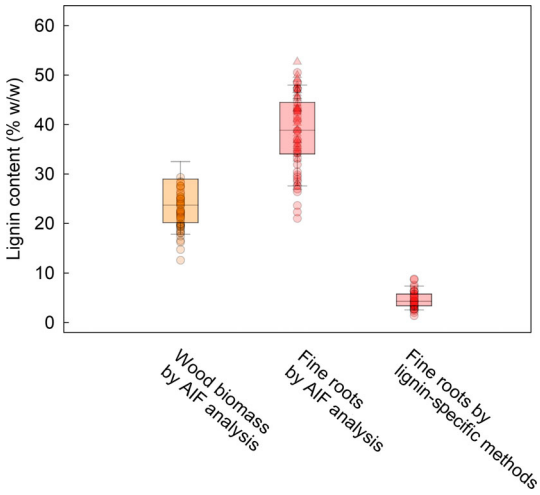

Fig. 6 Distribution of lignin content in wood biomass and fine roots across tree species. The lignin content of wood biomass (brown circles) was taken from published studies across 61 different biological wood samples from 25 genera spanning three major angiosperm clades (magnoliids, asterids and rosids, Table S8). The lignin content of fine roots determined by AIF analysis and lignin-specific methods (average of the estimates by CuO oxidation, thioacidolysis, and py-GC-MS) were measured in this study (red circles), with additional data points for lignin content from AIF analysis in fine roots obtained from a data synthesis published by Xia *et al*. (2015) that covers *c*. 30 temperate tree species from 14 genera (red triangles). The box plots show the median (horizontal line), the interquartile range (box), and the whiskers (extending to the 5th and 95th percentiles, respectively).

phylogenetically diverse tree species. Although the FTIR band at *c*. 1500 cm^{-1} proved to be a good lignin proxy in one, or a few, species (e.g. Xia *et al*., 2017), its relative intensity was not a good predictor of lignin content nor acid-insoluble fraction across chemically diverse root samples. When coupled with multivariate modeling, FTIR-ATR spectra showed moderate prediction power in its prediction of root lignin content, yet completely lacked the ability to predict lignin composition. The generally low degree of accuracy of FTIR-ATR in predicting root lignin may arise from the significant and variable matrix effects on the IR spectra of root samples across phylogenetically diverse tree species.

We acknowledge that the lignin-specific techniques also have their limitations (Table 1). The CuO reaction, thioacidolysis, and py-GC-MS are degradative methods that may modify the natural chemistry of lignin. Incomplete reaction and loss of lignin-derived products may also lead to underestimation when only phenolic monomers are used as standards for lignin quantification (Faust *et al*., 2018). Here we used mildly isolated lignin that largely keeps natural lignin linkages (Sette *et al*., 2011) as external lignin standards to calibrate for the recovery rate of lignin-derived monomers in each method. However, this did not account for any matrix effects that may occur individually for each chemically distinct sample. Using isotope-labeled lignin as an internal standard may further improve the accuracy of lignin quantification (e.g. van Erven *et al*., 2017). Another consideration is that we did not differentiate mycorrhizal fungal mass from root mass, so lignin content was measured on the basis of the mycorrhizal roots as a whole. The presence of fungal mass in roots may be probed and corrected by measuring ergosterol contents in roots (Ekblad *et al*., 1995). We note that our determination of lignin content on a mycorrhizal root basis is in line with current decomposition and biogeochemistry studies that commonly measure the biomass of mycorrhizal roots as the input of root litters to the soil.

Our data revealed a general disconnection between proximate and lignin-specific methods in their estimates of lignin content in fine roots across tree species and highlights the feasibility of py-GC-MS combined with predictive modeling as a fast-screening technique for describing the variation of lignin content and composition in fine roots. Overall, we evaluated the comparability and suitability of lignin analytical methods in fine roots across a broad range of tree species, which could provide a basis for the interpretation of root lignin data and help make informed methodology decisions for future studies.

Acknowledgements

This research is supported by funding from grants DEB 1754679 and DEB-1549964 from the U.S. National Science Foundation, and NIFA/USDA project number SC-1700597. Part of the analysis was supported by The National Institute of Food and Agriculture award 2021-70410-35296 to the Multi-User Analytical Laboratory at Clemson University. This is technical contribution No. 7096 of the Clemson University Experiment Station.

Author contributions

MX, OJV-B, CBB and NT conceived the idea. OJV-B and CBB determined the species that were included in this study, collected the samples, and performed root morphology analysis. MX, NT, performed chemical analysis. MX performed data analysis and wrote the draft of the manuscript, with critical feedback from OJV-B, VS, CBB and NT.

ORCID

Christopher B. Blackwood https://orcid.org/0000-0001-5764-6978
Vidya Suseela https://orcid.org/0000-0002-2934-4849
Nishanth Tharayil https://orcid.org/0000-0001-6866-0804
Oscar J. Valverde-Barrantes https://orcid.org/0000-0002-7327-7647
Mengxue Xia https://orcid.org/0000-0003-4366-3253

Data availability

The database that was used to generate phylogenetic relationships in this study can be found at http://www.onezoom.org/tree_index.html. The root morphology and acid-insoluble fraction data are deposited in the online data repository Dryad (doi: 10.5061/dryad.53mc6). The chemical data from other lignin methods are available upon request from the corresponding authors.

© 2022 The Authors
New Phytologist © 2022 New Phytologist Foundation.

References

Baker MJ, Trevisan J, Bassan P, Bhargava R, Butler HJ, Dorling KM, Fielden PR, Fogarty SW, Fullwood NJ, Heys KA. 2014. Using Fourier transform IR spectroscopy to analyze biological materials. *Nature Protocols* **9**: 1771–1791.

Bjorkman A. 1956. Studies on finely divided wood. Part 1. Extraction of lignin with neutral solvents. *Sven Papperstidn* **59**: 477–485.

Boerjan W, Ralph J, Baucher M. 2003. Lignin biosynthesis. *Annual Review of Plant Biology* **54**: 519–546.

Bujak R, Daghir-Wojtkowiak E, Kaliszan R, Markuszewski MJ. 2016. PLS-based and regularization-based methods for the selection of relevant variables in non-targeted metabolomics data. *Frontiers in Molecular Biosciences* **3**: 35.

Chen W, Koide RT, Adams TS, DeForest JL, Cheng L, Eissenstat DM. 2016. Root morphology and mycorrhizal symbioses together shape nutrient foraging strategies of temperate trees. *Proceedings of the National Academy of Sciences, USA* **113**: 8741–8746.

Dean JF. 1997. Lignin analysis. In: Dashek WV, ed. *Methods in plant biochemistry and molecular biology*. Boca Raton, FL, USA: CRC Press, 199–215.

Del Río JC, Rencoret J, Marques G, Li J, Gellerstedt G, Jimenez-Barbero J, Martinez AT, Gutiérrez A. 2009. Structural characterization of the lignin from jute (*Corchorus capsularis*) fibers. *Journal of Agricultural and Food Chemistry* **57**: 10271–10281.

Del Río JC, Rencoret J, Prinsen P, AnT M, Ralph J, Gutiérrez A. 2012. Structural characterization of wheat straw lignin as revealed by analytical pyrolysis, 2D-NMR, and reductive cleavage methods. *Journal of Agricultural and Food Chemistry* **60**: 5922–5935.

Ekblad AL, Wallander H, Carlsson R, Huss-Danell KE. 1995. Fungal biomass in roots and extramatrical mycelium in relation to macronutrients and plant biomass of ectomycorrhizal *Pinus sylvestris* and *Alnus incana*. *New Phytologist* **131**: 443–451.

Erler A, Riebe D, Beitz T, Löhmannsröben H-G, Gebbers R. 2020. Soil nutrient detection for precision agriculture using handheld laser-induced breakdown spectroscopy (LIBS) and multivariate regression methods (PLSR, Lasso and GPR). *Sensors* **20**: 418.

van Erven G, de Visser R, Merkx DW, Strolenberg W, de Gijsel P, Gruppen H, Kabel MA. 2017. Quantification of lignin and its structural features in plant biomass using 13C lignin as internal standard for pyrolysis-GC-SIM-MS. *Analytical Chemistry* **89**: 10907–10916.

van Erven G, Nayan N, Sonnenberg AS, Hendriks WH, Cone JW, Kabel MA. 2018. Mechanistic insight in the selective delignification of wheat straw by three white-rot fungal species through quantitative ^{13}C-IS py-GC-MS and whole cell wall HSQC NMR. *Biotechnology for Biofuels* **11**: 1–6.

Fahey LM, Nieuwoudt MK, Harris PJ. 2017. Predicting the cell-wall compositions of *Pinus radiata* (radiata pine) wood using ATR and transmission FTIR spectroscopies. *Cellulose* **24**: 5275–5293.

Fahmi R, Bridgwater A, Thain S, Donnison I, Morris P, Yates N. 2007. Prediction of Klason lignin and lignin thermal degradation products by Py-GC/MS in a collection of Lolium and Festuca grasses. *Journal of Analytical and Applied Pyrolysis* **80**: 16–23.

Faust S, Kaiser K, Wiedner K, Glaser B, Joergensen RG. 2018. Comparison of different methods for determining lignin concentration and quality in herbaceous and woody plant residues. *Plant and Soil* **433**: 7–18.

Filley TR, Nierop KG, Wang Y. 2006. The contribution of polyhydroxyl aromatic compounds to tetramethylammonium hydroxide lignin-based proxies. *Organic Geochemistry* **37**: 711–727.

Freschet GT, Cornwell WK, Wardle DA, Elumeeva TG, Liu W, Jackson BG, Onipchenko VG, Soudzilovskaia NA, Tao J, Cornelissen JH. 2013. Linking litter decomposition of above-and below-ground organs to plant–soil feedbacks worldwide. *Journal of Ecology* **101**: 943–952.

Gherardi LA, Sala OE. 2020. Global patterns and climatic controls of belowground net carbon fixation. *Proceedings of the National Academy of Sciences, USA* **117**: 20038–20043.

Ghetti P, Ricca L, Angelini L. 1996. Thermal analysis of biomass and corresponding pyrolysis products. *Fuel* **75**: 565–573.

Goñi MA, Nelson B, Blanchette RA, Hedges JI. 1993. Fungal degradation of wood lignins: geochemical perspectives from CuO-derived phenolic dimers and monomers. *Geochimica et Cosmochimica Acta* **57**: 3985–4002.

Guo D, Xia M, Wei X, Chang W, Liu Y, Wang Z. 2008. Anatomical traits associated with absorption and mycorrhizal colonization are linked to root branch order in twenty-three Chinese temperate tree species. *New Phytologist* **180**: 673–683.

Harman-Ware AE, Foster C, Happs RM, Doeppke C, Meunier K, Gehan J, Yue F, Lu F, Davis MF. 2016. A thioacidolysis method tailored for higher-throughput quantitative analysis of lignin monomers. *Biotechnology Journal* **11**: 1268–1273.

Hedges JI, Ertel JR. 1982. Characterization of lignin by gas capillary chromatography of cupric oxide oxidation products. *Analytical Chemistry* **54**: 174–178.

Horikawa Y, Hirano S, Mihashi A, Kobayashi Y, Zhai S, Sugiyama J. 2019. Prediction of lignin contents from infrared spectroscopy: chemical digestion and lignin/biomass ratios of Cryptomeria japonica. *Applied Biochemistry and Biotechnology* **188**: 1066–1076.

Iversen C, Powell A, McCormack M, Blackwood C, Freschet G, Kattge J, Roumet C, Stover D, Soudzilovskaia N, Valverde-Barrantes O. 2017. *Fine-Root Ecology Database (FRED): a global collection of root trait data with coincident site, vegetation, edaphic, and climatic data, v.1*. Oak Ridge, TN, USA: Oak Ridge National Laboratory, TES SFA, U.S. Department of Energy.

Jurak E, Punt AM, Arts W, Kabel MA, Gruppen H. 2015. Fate of carbohydrates and lignin during composting and mycelium growth of *Agaricus bisporus* on wheat straw based compost. *PLoS ONE* **10**: e0138909.

Kleen M, Lindblad G, Backa S. 1993. Quantification of lignin and carbohydrates in kraft pulps using analytical pyrolysis and multivariate data analysis. *Journal of Analytical and Applied Pyrolysis* **25**: 209–227.

Lapierre C. 1993. Application of new methods for the investigation of lignin structure. In: *Forage cell wall structure and digestibility, vol. 1*. Madison, WI, USA: American Society of Agronomy, 133–166.

Leuschner C, Coners H, Icke R, Hartmann K, Effinger ND, Schreiber L. 2003. Chemical composition of the periderm in relation to in situ water absorption rates of oak, beech and spruce fine roots. *Annals of Forest Science* **60**: 763–772.

McCormack ML, Dickie IA, Eissenstat DM, Fahey TJ, Fernandez CW, Guo D, Helmisaari HS, Hobbie EA, Iversen CM, Jackson RB. 2015. Redefining fine roots improves understanding of below-ground contributions to terrestrial biosphere processes. *New Phytologist* **207**: 505–518.

Muggeo VM. 2008. SEGMENTED: an R package to fit regression models with broken-line relationships. *R News* **8**: 20–25.

Müller G, Schöpper C, Vos H, Kharazipour A, Polle A. 2009. FTIR-ATR spectroscopic analyses of changes in wood properties during particle-and fibreboard production of hard-and softwood trees. *BioResources* **4**: 49–71.

Pandey K, Pitman A. 2003. FTIR studies of the changes in wood chemistry following decay by brown-rot and white-rot fungi. *International Biodeterioration & Biodegradation* **52**: 151–160.

Pandey KK, Pitman AJ. 2004. Examination of the lignin content in a softwood and a hardwood decayed by a brown-rot fungus with the acetyl bromide method and Fourier transform infrared spectroscopy. *Journal of Polymer Science Part A: Polymer Chemistry* **42**: 2340–2346.

Parthasarathi R, Romero RA, Redondo A, Gnanakaran S. 2011. Theoretical study of the remarkably diverse linkages in lignin. *The Journal of Physical Chemistry Letters* **2**: 2660–2666.

Preston CM, Nault JR, Trofymow J. 2009. Chemical changes during 6 years of decomposition of 11 litters in some Canadian forest sites. Part 2. 13 C abundance, solid-state 13 C NMR spectroscopy and the meaning of "lignin". *Ecosystems* **12**: 1078–1102.

Ralph J, Hatfield RD. 1991. Pyrolysis-GC-MS characterization of forage materials. *Journal of Agricultural and Food Chemistry* **39**: 1426–1437.

Ralph J, Lundquist K, Brunow G, Lu F, Kim H, Schatz PF, Marita JM, Hatfield RD, Ralph SA, Christensen JH *et al.* 2004. Lignins: natural polymers from oxidative coupling of 4-hydroxyphenyl-propanoids. *Phytochemistry Reviews* **3**: 29–60.

Rasse DP, Rumpel C, Dignac M-F. 2005. Is soil carbon mostly root carbon? Mechanisms for a specific stabilisation. *Plant and Soil* **269**: 341–356.

Reyt G, Ramakrishna P, Salas-González I, Fujita S, Love A, Tiemessen D, Lapierre C, Morreel K, Calvo-Polanco M, Flis P *et al.* 2021. Two chemically distinct root lignin barriers control solute and water balance. *Nature Communications* **12**: 1–5.

Rodrigues J, Faix O, Pereira H. 1998. Determination of lignin content of Eucalyptus globulus wood using FTIR spectroscopy. *Holzforschung* **52**: 46–50.

© 2022 The Authors
New Phytologist © 2022 New Phytologist Foundation.

Rolando C, Monties B, Lapierre C. 1992. Thioacidolysis. In: Lin SY, Dence CW, eds. *Methods in lignin chemistry*. Springer series in wood science. Berlin, Germany: Springer, 334–349.

Ryan MG, Melillo JM, Ricca A. 1990. A comparison of methods for determining proximate carbon fractions of forest litter. *Canadian Journal of Forest Research* **20**: 166–171.

Schneider HM, Strock CF, Hanlon MT, Vanhees DJ, Perkins AC, Ajmera IB, Sidhu JS, Mooney SJ, Brown KM, Lynch JP. 2021. Multiseriate cortical sclerenchyma enhance root penetration in compacted soils. *Proceedings of the National Academy of Sciences, USA* **118**: e2012087118.

See CR, Luke McCormack M, Hobbie SE, Flores-Moreno H, Silver WL, Kennedy PG. 2019. Global patterns in fine root decomposition: climate, chemistry, mycorrhizal association and woodiness. *Ecology Letters* **22**: 946–953.

Senior JK, Potts BM, Davies NW, Wooliver RC, Schweitzer JA, Bailey JK, O'Reilly-Wapstra JM. 2016. Phylogeny explains variation in the root chemistry of Eucalyptus species. *Journal of Chemical Ecology* **42**: 1086–1097.

Sette M, Wechselberger R, Crestini C. 2011. Elucidation of lignin structure by quantitative 2D NMR. *Chemistry–A European Journal* **17**: 9529–9535.

Simard SW, Beiler KJ, Bingham MA, Deslippe JR, Philip LJ, Teste FP. 2012. Mycorrhizal networks: mechanisms, ecology and modelling. *Fungal Biology Reviews* **26**: 39–60.

Sluiter JB, Ruiz RO, Scarlata CJ, Sluiter AD, Templeton DW. 2010. Compositional analysis of lignocellulosic feedstocks. 1. Review and description of methods. *Journal of Agricultural and Food Chemistry* **58**: 9043–9053.

Smith BC. 2011. *Fundamentals of Fourier transform infrared spectroscopy*. Boca Raton, FL, USA: CRC Press.

Solly EF, Schöning I, Boch S, Kandeler E, Marhan S, Michalzik B, Müller J, Zscheischler J, Trumbore SE, Schrumpf M. 2014. Factors controlling decomposition rates of fine root litter in temperate forests and grasslands. *Plant and Soil* **382**: 203–218.

Soukup A, Mala J, Hrubcova M, Kalal J, Votrubova O, Cvikrova M. 2004. Differences in anatomical structure and lignin content of roots of pedunculate oak and wild cherry-tree plantlets during acclimation. *Biologia Plantarum* **48**: 481–489.

Sun T, Hobbie SE, Berg B, Zhang H, Wang Q, Wang Z, Hattenschwiler S. 2018. Contrasting dynamics and trait controls in first-order root compared with leaf litter decomposition. *Proceedings of the National Academy of Sciences, USA* **115**: 10392–10397.

Suseela V, Tharayil N. 2018. Decoupling the direct and indirect effects of climate on plant litter decomposition: accounting for stress-induced modifications in plant chemistry. *Global Change Biology* **24**: 1428–1451.

Suseela V, Tharayil N, Orr G, Hu D. 2020. Chemical plasticity in the fine root construct of *Quercus* spp. varies with root order and drought. *New Phytologist* **228**: 1835–1851.

Talbot JM, Yelle DJ, Nowick J, Treseder KK. 2012. Litter decay rates are determined by lignin chemistry. *Biogeochemistry* **108**: 279–295.

Taylor BR, Parkinson D, Parsons WF. 1989. Nitrogen and lignin content as predictors of litter decay rates: a microcosm test. *Ecology* **70**: 97–104.

Valverde-Barrantes OJ, Smemo KA, Blackwood CB. 2015. Fine root morphology is phylogenetically structured, but nitrogen is related to the plant economics spectrum in temperate trees. *Functional Ecology* **29**: 796–807.

Wang JJ, Tharayil N, Chow AT, Suseela V, Zeng H. 2015. Phenolic profile within the fine-root branching orders of an evergreen species highlights a disconnect in root tissue quality predicted by elemental- and molecular-level carbon composition. *The New Phytologist* **206**: 1261–1273.

Wold S, Sjöström M, Eriksson L. 2001. PLS-regression: a basic tool of chemometrics. *Chemometrics and Intelligent Laboratory Systems* **58**: 109–130.

Xia M, Talhelm AF, Pregitzer KS. 2015. Fine roots are the dominant source of recalcitrant plant litter in sugar maple-dominated northern hardwood forests. *New Phytologist* **208**: 715–726.

Xia M, Talhelm AF, Pregitzer KS. 2017. Chronic nitrogen deposition influences the chemical dynamics of leaf litter and fine roots during decomposition. *Soil Biology and Biochemistry* **112**: 24–34.

Xia M, Valverde-Barrantes OJ, Suseela V, Blackwood CB, Tharayil N. 2021. Coordination between compound-specific chemistry and morphology in plant roots aligns with ancestral mycorrhizal association in woody angiosperms. *New Phytologist* **232**: 1259–1271.

Yue F, Lu F, Sun R-C, Ralph J. 2012. Syntheses of lignin-derived thioacidolysis monomers and their uses as quantitation standards. *Journal of Agricultural and Food Chemistry* **60**: 922–928.

Zanne AE, Tank DC, Cornwell WK, Eastman JM, Smith SA, FitzJohn RG, McGlinn DJ, O'Meara BC, Moles AT, Reich PB *et al.* 2014. Three keys to the radiation of angiosperms into freezing environments. *Nature* **506**: 89–92.

Supporting Information

Additional Supporting Information may be found online in the Supporting Information section at the end of the article.

Fig. S1 Relative abundance of 4-vinylguaiacol vs G-type lignin and 4-vinylphenol vs total lignin estimated by pyrolysis–gas chromatography–mass spectrometry, and the ratio of cell-wall bound hydroxycinnamates : total lignin (w/w) in fine roots across 34 tree species.

Fig. S2 Least absolute shrinkage and selection operator model fittings and external validation for the prediction of lignin content and monomeric composition in fine roots across tree species, based on high-throughput techniques.

Table S1 Root samples from 34 tree species at two study sites analyzed using five lignin analytical methods.

Table S2 Retention times and characteristic mass fragments of 14 authentic phenol standards.

Table S3 The pyrolysis products of lignin and their signature fragments used in pyrolysis–gas chromatography–mass spectrometry for lignin characterization.

Table S4 Method performance of the copper oxide reaction, thioacidolysis, and pyrolysis–gas chromatography–mass spectrometry methods for quantifying lignin content and monomer composition.

Table S5 The pyrolysis products selected by least absolute shrinkage and selection operator that are predictors of lignin abundance in fine roots across tree species.

Table S6 The pyrolysis products selected by least absolute shrinkage and selection operator that are predictors of the S : G ratio (an indicator of lignin monomeric composition) in fine roots across tree species.

Table S7 Fourier transform infrared spectroscopy wavenumbers selected by least absolute shrinkage and selection operator that are predictors of lignin abundance in fine roots across tree species.

Table S8 The acid-insoluble fraction (AIF, or Klason lignin) content in wood biomass across angiosperm tree species.

Please note: Wiley is not responsible for the content or functionality of any Supporting Information supplied by the authors. Any queries (other than missing material) should be directed to the *New Phytologist* Central Office.

© 2022 The Authors
New Phytologist © 2022 New Phytologist Foundation.